THE IMPACT OF CO_2-BRINE INTERFACIAL TENSION ON THE RELATIVE PERMEABILITY OF THE CO_2-BRINE-SANDSTONE SYSTEM AT RESERVOIR CONDITIONS

Catriona Reynolds, Martin Blunt, Sam Krevor
Department of Earth Science and Engineering, Imperial College London

This paper was prepared for presentation at the International Symposium of the Society of Core Analysts held in Napa Valley, California, USA, 16-19 September, 2013.

ABSTRACT

In geologic CO_2 storage the flow of CO_2 once injected and how much of the CO_2 can be trapped relies on the relative permeability of each phase. The flow and distribution of CO_2 in the pore-space is controlled by CO_2-brine interfaces and the interfacial tension (IFT) between the phases. In oil-brine systems, the relative permeability is known to depend on the IFT only at values less than 1mN m^{-1}, but the effect on CO_2-brine systems is unknown. Additionally, the IFT of CO_2-brine systems are well characterized across the range of subsurface conditions and varies widely, from 25 to 55 mN m^{-1}. A program of steady-state core floods is planned to measure relative permeability curves for drainage and imbibition at interfacial tensions of 28 to 49 mN m^{-1}, at pressure, temperature and salinity conditions relevant to the storage of supercritical CO_2 (8-25 MPa, 35-120˚C and 0-5 mol kg^{-1}). Conditions are selected so as to varying interfacial tension over the temperature, pressure and salinity conditions pertinent to CO_2 storage, while minimizing the variation in viscosity ratio between CO_2 and brine.

We present the first result of an experimental investigation into the impact of the CO_2-brine interfacial tension on the relative permeability of the CO_2-brine-sandstone system for an interfacial tension of 36 mNm^{-1} at 100˚C and 11.2 MPa. Additionally we highlight the use of multiphase flow theory to plan steady state core floods, particularly when aiming for high CO_2 saturations during drainage.

The work is performed in a high pressure, high temperature core-flooding and x-ray imaging facility recently built at Imperial College London for the investigation of multiphase flow and CO_2 storage. Experiments are performed on Bentheimer sandstone, using a comprehensive suite of core flood techniques, combining traditional steady state and novel techniques to obtain permeabilities at high CO_2 saturations. In situ fluid saturations are measured using an X-ray CT scanner.

INTRODUCTION

The flow and distribution of fluids in porous media are controlled by fluid-fluid interfaces. The interfaces are characterised by the interfacial tension, where varying the IFT will change the capillary pressure and relative permeability in each phase [1]-[3]. The ultimate distribution of residually trapped CO_2 is a function of the hysteresis in relative permeability between drainage and imbibition, which are in turn a function of the rock and fluid properties, as well as pressure and temperature conditions in the reservoir [4], [5]. Characteristic curves for relative permeability are a fundamental input to reservoir simulators that can be used both to history match and to design storage projects. Hence, accurate measurements of relative permeability at the conditions relevant to CO_2 storage are vital to be able to predict the migration of a plume of CO_2 once injected into the subsurface and the volumes of CO_2 that can be trapped by capillary snap-off.

Despite increased interest in CO_2 storage, the response of the CO_2-water relative permeability to varying IFT has yet to be comprehensively evaluated, as has the impact on residual trapping.

INTERFACIAL TENSION IN THE OIL-BRINE SYSTEM

Much of the work investigating the effect of interfacial tension on relative permeability in the oil-brine system is motivated by enhanced oil recovery, where the goal is to reduce the oil-water interfacial tension by adding surfactants, in order to approximate miscible flow and reduce the residual saturation of oil. Interfacial tension is observed to have no impact on relative permeability in the oil-brine system at tensions above 1 mN m^{-1} [6], with no real measurable change until interfacial tensions drop below 10^{-3} mN m^{-1}. Below this point relative permeability increases dramatically for decreasing interfacial tension. Relative permeability curves straighten, hysteresis effects diminish and residual saturations tend to zero, as the flow between oil and water approaches miscible behaviour [1], [3], [7].

The interfacial tension on the CO_2-brine system is well characterised across the temperature, pressure and salinity range relevant to geologic CO_2 storage. Values range from 25-55 mN m^{-1}, decreasing with increasing pressure and salinity, and increasing with increasing temperature [8]. Comparison with oil-brine systems would suggest that at such high interfacial tensions there should be no observable change in relative permeability. However, Bachu and Bennion [9] suggest this is not the case. They observe a significant increase in relative permeability for drainage and imbibition over a range of interfacial tensions of 19.8 to 56.2 mN m^{-1} in a water-wet sandstone.

SELECTION OF CONDITIONS

The experimental conditions are chosen so as to represent the range of interfacial tensions that may be encountered for geological storage or supercritical CO_2 in a typical saline aquifer. Temperature and pressure ranges from 305 to 395 K and 7.5 to 30 MPa, corresponding to depth of ~1 to 3 km, where the minimum pressure and temperature are

above the critical point for CO_2 (T_c = 304 K and P_c = 7.38 MPa). The salinity of formation brines range from 50 000 to 400 000 mg l^{-1} [10] or 0.8 to 6.5 mol kg^{-1} globally.

The change in fluid properties such as viscosity and interfacial tension with pressure, temperature and salinity in the CO_2-brine system are well known [8], [11], [12]. Interfacial tension varies from 25 to 55 mN m^{-1}, while viscosity ratio, $M = \mu_{CO_2}/\mu_w$, ranges from 0.02 to 0.2, with most of the change coming from μ_{CO_2} [13], [14].

Conditions may be easily selected to obtain a range of interfacial tensions. However, isolating the independent impact of interfacial tension on relative permeability is less simple. As a result, it is common to use a dimensionless parameter such as the capillary number,

$$N_c = \frac{q\mu}{\gamma}, \quad (1)$$

where q is the Darcy fluid velocity, μ is the viscosity of the displacing fluid and γ is the interfacial tension, to describe the combined effects of interfacial tension and viscosity on relative permeability for different temperature, pressure and salinity conditions [1]-[3], [9].

It is not clear what effect viscosity has on relative permeability. The oil-brine system is characterised by a high viscosity ratio ($M \gg 1$), and experimental evidence suggests relative permeability may be independent of [15], increase [16]-[18], or decrease [19] with viscosity ratio. In contrast, the CO_2-brine system is characterised by a low viscosity ratio ($M \ll 1$). Bachu and Bennion find decreasing the viscosity ratio (from 0.1 to 0.02) reduces the relative permeability, but note that they are unable to separate this from the effect of increasing interfacial tension (from 19.8 to 56.2 mN m^{-1}) [9], [20], [21].

To ensure greater clarity in the interpretation of our results, where possible we select conditions along lines of constant viscosity ratio so as to isolate the effect of interfacial tension (Figure 1).

EXPERIMENTAL PROCEDURE

Relative permeability is measured using the steady-state method on horizontal core floods. Supercritical CO_2 and brine are circulated through the core at a constant total volumetric flow rate. The fluids are saturated with respect to one another, to ensure displacement is immiscible. Pressure is measured at the inlet and outlet faces of the core. Fluids are circulated through the core until the fluid saturations in the core reaches steady state and the pressure drop stabilises. To measure the primary drainage relative permeability, flow of CO_2 is increased stepwise from zero to 100% (with water reduced concurrently), until maximum CO_2 saturation is achieved.

Under the conditions of a horizontal, steady state core flood, the relative permeability of each phase may be calculated using the multiphase extension to Darcy's Law [22],

$$q_i = -\frac{Akk_{r,i}S_i}{\mu_i}\frac{\Delta P}{L}, \quad (2)$$

where the cross-sectional area, A, and length, L, of the core, and absolute permeability k are measured prior to beginning the experiment. For each fluid phase (subscript i) the flow rate q_i is specified and viscosity μ_i is calculated for the experimental conditions. For each change in flow rate, the relative permeability $k_{r,i}$ can be obtained from the measured pressure drop ($\Delta P = P_{inlet} - P_{outlet}$) across the core and in situ fluid saturation S_i is observed using an x-ray CT scanner. All flow lines, pumps and the core are heated to the desired experimental temperature and a back pressure pump on the outlet side of the core is used to maintain the pressure.

USING MULTIPHASE FLOW THEORY FOR EXPERIMENTAL DESIGN

The Buckley Leverett equation is used to calculate relative permeability in unsteady state core floods. However, the equation may also be used to design steady state core floods. In particular, to obtain specific saturations in the core and to estimate the time taken to reach steady state saturation at a particular fractional flow. Although not a new technique, the procedure is not a routine part of steady state core flooding, and thus is reviewed in the following section.

The Buckley Leverett solution for forced displacement [23] is given as follows:

$$\frac{dx_D}{dt_D} = \frac{df_{CO_2}}{dS_{CO_2}} \quad (3)$$

and

$$\frac{dS_{CO_2}}{dt_D} = 0. \quad (4)$$

Graphically, Equations 3 and 4 are represented by lines of constant S_{CO_2} in x_D-t_D space which have a slope of gradient df_{CO_2}/dS_{CO_2}. In terms of a core flood experiment, each f_{CO_2} has an associated steady state S_{CO_2}. When a particular fractional flow is selected, the saturation at the inlet of core immediately increases to the steady state level. This saturation then proceeds along the length of the core at a velocity given by the slope of the fractional flow curve. Thus the time taken to reach steady state can be calculated from the velocity by converting back from dimensionless parameter space (Figure 2). Multiphase flow theory may be used in such a way to estimate the saturation that should be achieved for each fractional flow and the time taken to reach steady state at each step. However, this requires some a priori knowledge as to the shape of the fractional flow curve.

The usual method for creating a drainage relative permeability curve using the steady state method is to pick some fractional flow of CO_2, wait until the pressure drop across the core stabilises, then measure the saturation and calculate the relative permeability using Equation 2. The f_{CO_2} is then increased incrementally for a constant q_T, each time waiting for a steady state saturation to be achieved. At the end of the experiment, curves may be fitted to the data using relative permeability relationships, such as the Brooks-Corey equation,

$$k_{r,nw} = k_{r,nw(S_{w,irr})}(1 - S_w^*)^2(1 - S_w^{*\,n}) \tag{5}$$

and

$$k_{r,w} = S_w^{*\,m}, \tag{6}$$

where the reduced saturation is given by $S_w^* = \left(S_w - S_{w,irr}\right)/\left(1 - S_{w,irr}\right)$ [24], [25].

By this method there is no knowledge of the saturation that may be achieved at each step. Consequently it is easy to pick too large or too small a change in fractional flow, which can result in an unsatisfactory range of data points from which to build the relative permeability curves.

If other measurements of relative permeability or some knowledge as to the wetting properties of the rock are known, first guess relative permeability curves can be created by choosing appropriate values for $n, m, S_{w,irr}$ and $k_{r,nw(S_{w,irr})}$, and a fractional flow curve plotted using the reduced fractional flow formulation $f_{CO_2} = \lambda_{CO_2}/\lambda_T$, where $\lambda_i = k_{r,i}/\mu_i$ and $\lambda_T = \lambda_w + \lambda_{CO_2}$. The curves may then be used to pick fractional flows based on the desired saturation. As the core flood progresses, the parameters used to generate the relative permeability curves may be updated so as to improve the prediction (Figure 3).

There are two main benefits to carrying out a core flood in this way: first, fractional flows may be selected to as to control the range of saturations over which relative permeability is measured; and second, predictions can be made as to the time to reach steady state for each step. This is of particular importance when trying to achieve a high CO_2 saturation in the core, when the choice between an f_{CO_2} of 0.9990 or 0.9995 can make difference between achieving an S_{CO_2} of 0.6 in a few hours, or 0.7 in a few days (Figure 2).

RESULTS OF FIRST CORE FLOOD

Drainage relative permeability curves and calculated relative permeability for the first in a program of eight steady-state core flood experiments are shown in Figure 4 and Table 1. Rock and fluid parameters are given in Tables 2 and 3. The slice-averaged saturation (from x-ray CT) is shown in Figure 5. Saturation profiles are mostly consistent, with an increase of ~10% towards the outlet, indicating a gradient in capillary pressure across the

core. Additionally, profile D6 shows a steep increase in S_w at the outlet of the core. This may be due to end effects or, more likely, because the equilibrium saturation front had not propagated the full length of the core and the steady saturation had not been reached.

RECCOMMENDATIONS

Future core floods should make use of the method outlined to predict the saturation achievable at each fractional flow to enable the measurement of relative permeability at high CO_2 saturations.

ACKNOWLEDGEMENTS

The authors gratefully acknowledge funding from the Qatar Carbonates and Carbon Storage Research Centre (QCCSRC), provided jointly by Qatar Petroleum, Shell, and Qatar Science & Technology Park and the Department of Earth Science & Engineering at Imperial College London

REFERENCES

[1] J. O. Amaefule and L. L. Handy, "The Effect of Interfacial Tensions on Relative Oil/Water Permeabilities of Consolidated Porous Media," *Old SPE Journal*, vol. 22, no. 3, pp. 371–381, Jun. 1982.

[2] C. Bardon and D. G. Longeron, "Influence of Very Low Interfacial Tensions on Relative Permeability," *Old SPE Journal*, vol. 20, no. 5, pp. 391–401, 1980.

[3] R. A. Fulcher Jr, T. Ertekin, and C. D. Stahl, "Effect of Capillary Number and Its Constituents on Two-Phase Relative Permeability Curves," *Journal of Petroleum Technology*, vol. 37, no. 2, pp. 249–260, Feb. 1985.

[4] R. Juanes, E. J. Spiteri, F. M. Orr Jr, and M. J. Blunt, "Impact of relative permeability hysteresis on geological CO_2 storage," *Water Resources Research*, vol. 42, no. 12, pp. 1–13, Dec. 2006.

[5] E. Spiteri, R. Juanes, M. Blunt, and F. Orr, "Relative-Permeability Hysteresis: Trapping Models and Application to Geological CO2 Sequestration," 2005.

[6] M. J. Oak, L. E. Baker, and D. C. Thomas, "Three-phase relative permeability of Berea sandstone," *Journal of Petroleum Technology*, vol. 42, no. 8, pp. 1054–1061, 1990.

[7] J. Batycky and F. McCaffery, "Low interfacial tension displacement studies," presented at the Annual Technical Meeting, 1978.

[8] X. Li, E. Boek, G. C. Maitland, and J. P. M. Trusler, "Interfacial Tension of (Brines + CO_2): (0.864 NaCl + 0.136 KCl) at Temperatures between (298 and 448) K, Pressures between (2 and 50) MPa, and Total Molalities of (1 to 5) $molkg^{-1}$," *Journal of Chemical & Engineering Data*, vol. 57, no. 4, pp. 1078–1088, Apr. 2012.

[9] S. Bachu and B. Bennion, "Effects of in-situ conditions on relative permeability characteristics of CO_2-brine systems," *Environmental Geology*, vol. 54, no. 8, pp. 1707–1722, 2008.

[10] J. S. Hanor, "Origin of saline fluids in sedimentary basins," *Geological Society,*

London, Special Publications, vol. 78, no. 1, pp. 151–174, Jan. 1994.

[11] J. Kestin, H. E. Khalifa, and R. J. Correia, "Tables of the Dynamic and Kinematic Viscosity of Aqueous NaCl Solutions in the Temperature Range 20-150°C and the Pressure Range 0.1-35 MPa," *American Chemical Society and the American Institute of Physics for the National Bureau of Standards*, pp. 1–17, 1981.

[12] A. Fenghour, W. A. Wakeham, and V. Vesovic, "The Viscosity of Carbon Dioxide," *Journal of Physical and Chemical Reference Data*, vol. 27, no. 1, pp. 31–44, 1998.

[13] J. J. Adams and S. Bachu, "Equations of state for basin geofluids: algorithm review and intercomparison for brines," *Geofluids*, vol. 2, pp. 257–271, Oct. 2002.

[14] J. M. Nordbotten, M. A. Celia, and S. Bachu, "Injection and Storage of CO_2 in Deep Saline Aquifers: Analytical Solution for CO_2 Plume Evolution During Injection," *Transport in Porous Media*, vol. 58, no. 3, pp. 339–360, Mar. 2005.

[15] M. C. LEverett, "Flow of oil-water mixtures through unconsolidated sands," *Trans., AIME*, vol. 132, p. 149, 1939.

[16] S. T. Yuster, "Theoretical considerations of multiphase flow in idealized capillary systems," vol. 2, pp. 437–445, 1951.

[17] A. S. Odeh, "The Effect of Viscosity Ratio on Relative Permeability," *Trans., AIME*, vol. 216, 1959.

[18] R. Ehrlich, "Viscous coupling in two-phase flow in porous media and its effect on relative permeabilities," *Transport in Porous Media*, vol. 11, no. 3, pp. 201–218, 1993.

[19] E. J. Lefebvre du Prey, "Factors Affecting Liquid-Liquid Relative Permeabilities of a Consolidated Porous Medium," *Old SPE Journal*, vol. 13, no. 1, pp. 39–47, Feb. 1973.

[20] D. B. Bennion and S. Bachu, "Drainage and Imbibition Relative Permeability Relationships for Supercritical CO_2/Brine and H_2S/Brine Systems in Intergranular Sandstone, Carbonate, Shale, and Anhydrite Rocks," *SPE Reservoir Evaluation and Engineering*, vol. 11, no. 3, pp. 487–496, Jun. 2008.

[21] D. Bennion and S. Bachu, "Dependence on temperature, pressure, and salinity of the IFT and relative permeability displacement characteristics of CO2 injected in deep saline aquifers," 2006.

[22] M. Muskat and M. W. Meres, "The Flow of Heterogeneous Fluids Through Porous Media," *Physics*, vol. 7, no. 9, pp. 346–363, 1936.

[23] S. E. Buckley and M. C. LEverett, "Mechanism of Fluid Displacement in Sands," *Trans., AIME*, vol. 146, no. 1, pp. 107–116, 1942.

[24] A. T. Corey, "The Interrelation Between Gas and Oil Relative Permeabilities," *Producers Monthly*, vol. 19, no. 1, pp. 38–41, 1954.

[25] M. M. Honarpour, L. Koederitz, and A. H. Harvey, *Relative Permeability of Petroleum Reservoirs*. CRC Press Ltd., 1986.

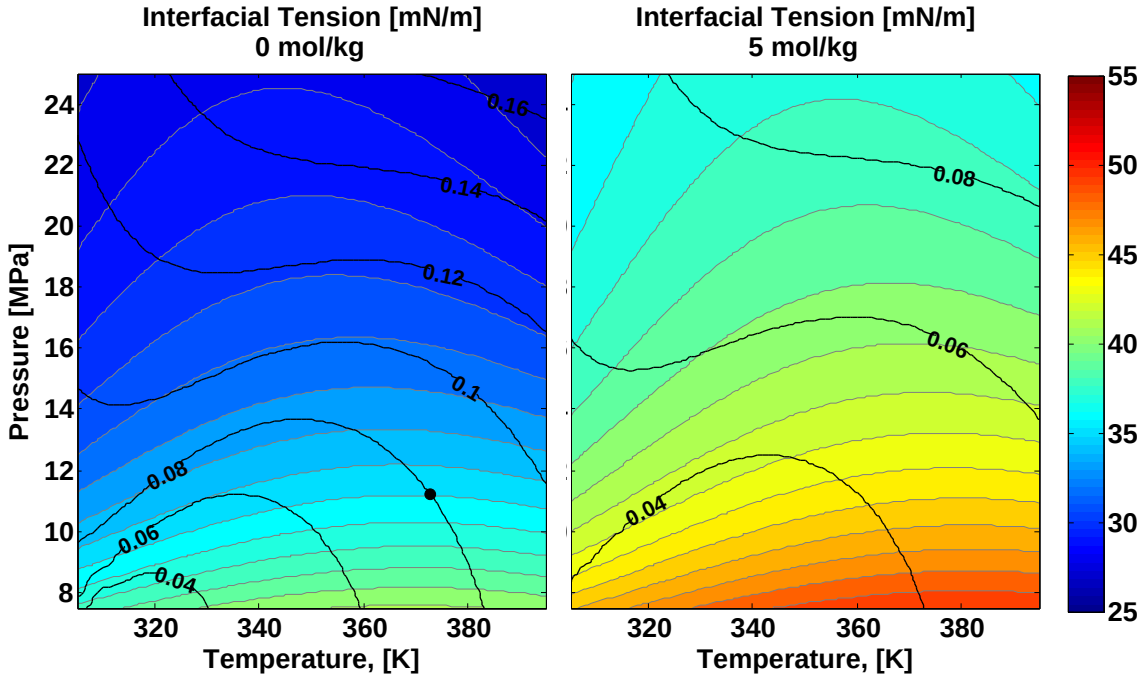

Figure 1. Interfacial tension varies from 25 to 55 mN m^{-1} over the pressure and temperature conditions relevant to geological CO_2 storage, for 0 and 5 mol kg^{-1} NaCl brine [8]. Black lines show calculated viscosity ratio M. The condition for the core flood presented in this paper is shown by the black dot.

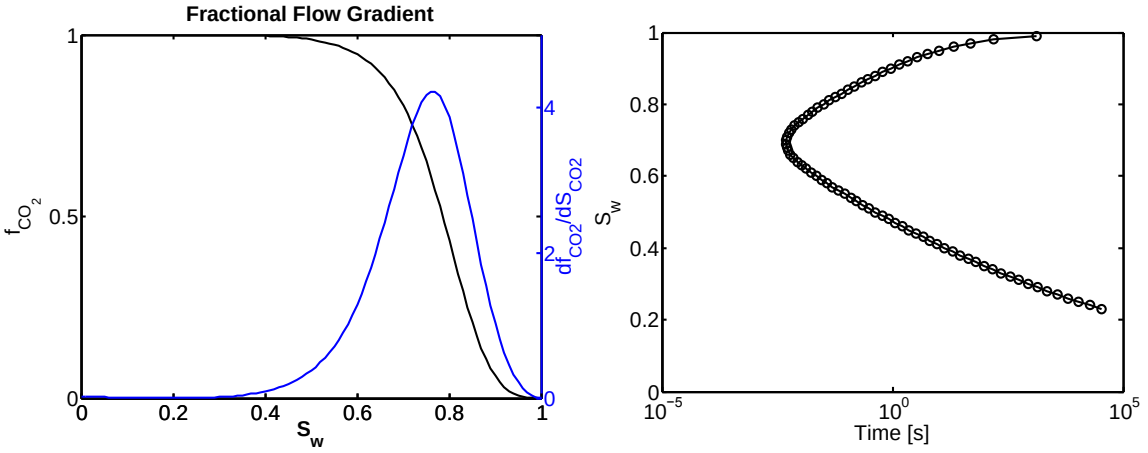

Figure 2. Left: The gradient of the fractional flow curve (blue) increases to a maximum as S_w decreases from 1 to ~0.75. Beyond this saturation the gradient decreases, thus the time taken to reach steady state will increase for high S_{CO2}. Right: For a typical fractional flow

curve between CO_2 and water in a water-wet core, the time taken for each saturation to travel across the core ranges over five orders of magnitude, from seconds to days.

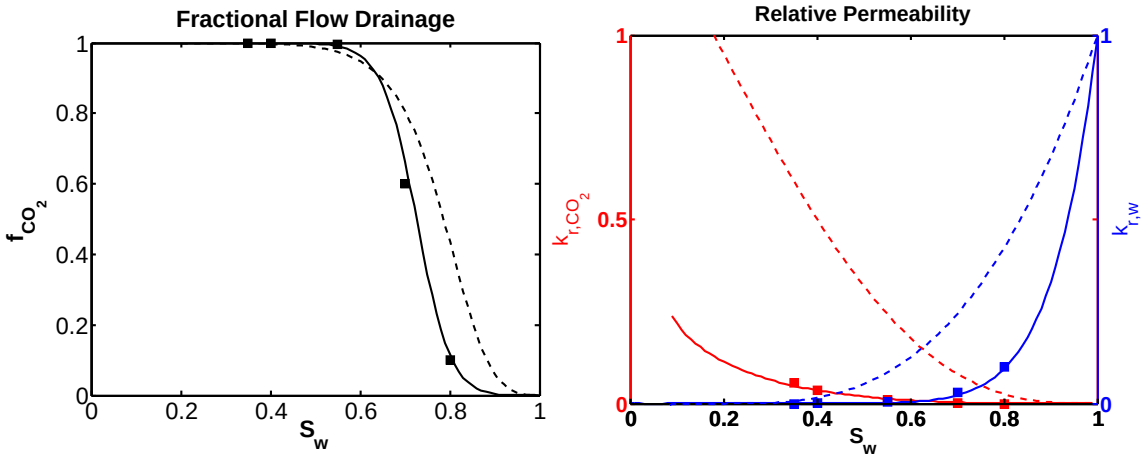

Figure 3. First guess relative permeability and fractional flow curves (dashed lines) may be predicted using a priori knowledge of the likely relative permeability and wetting properties of a core. These may then be updated (solid lines) as the core flood progresses and data points (solid squares) are obtained.

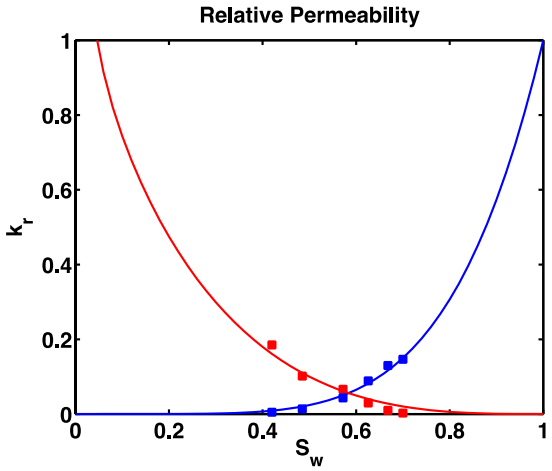

Figure 4. Measure drainage relative permeability (squares). Curves fit with Brooks-Corey parameters $n = 0.6, m = 5, S_{w,irr} = 0.05$ and $k_{r,nw(S_{w,irr})} = 1$.

Table 1. Relative permeability calculated from average saturation measured using an x-ray CT scanner and measured pressure drop across the core.

	S_w [-]	ΔP [bar]	f_{CO2} [-]	q_{CO2} [ml min^{-1}]	q_w [ml min^{-1}]	k_{CO2} [-]	k_w [-]
D1	0.700	0.5753	0.1730	3.460	16.540	0.00228	0.13629
D2	0.668	0.4032	0.4859	9.718	10.282	0.00915	0.12087
D3	0.626	0.2200	0.8082	16.164	3.836	0.02788	0.08265
D4	0.572	0.1171	0.9504	19.008	0.992	0.06158	0.04014
D5	0.485	0.0794	0.9892	19.784	0.216	0.09452	0.01289
D6	0.422	0.0440	0.9979	19.958	0.042	0.17212	0.00452

Table 2. Bentheimer core parameters

ϕ [-]	k [D]	L [m]	A [m^2]	q_T [ml min^{-1}]	V_p [ml]
0.2	1.98	0.239	0.00112	20	53.8

Table 3. Conditions of core flood and fluid parameters

S [mol kg^{-1}]	IFT [mN m^{-1}]	M [-]	T [K]	P [MPa]	ρ_{CO2} [kg m^3]	ρ_w [kg m^3]	μ_{CO2} [Pa s]	μ_w [Pa s]
0	36.0	0.08	373	11.2	220.17	963.59	0.00002285	0.000285389

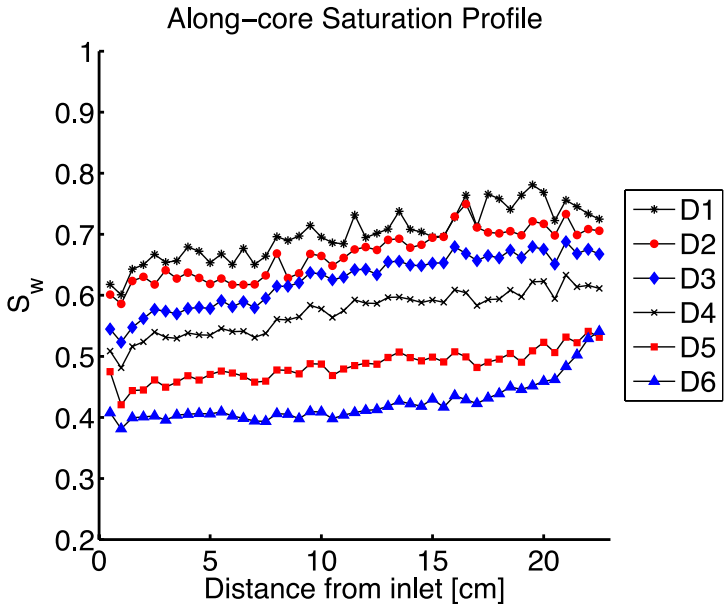

Figure 5. Slice-averaged saturation (CT) in the core.